Calibration of a tibia-based phase variable for control of robotic transtibial prostheses

Ryan R. Posh[1], Jonathan A. Tittle[1], James P. Schmiedeler[1], and Patrick M. Wensing[1]

***Abstract*— Phase variable control based on global tibia kinematics holds promise for predicting gait cycle progression to continuously control robotic transtibial prostheses. Calibration of the phase variable is critical to ensure its monotonic behavior, to approach a linear relationship with gait percentage, and to accurately predict the percentage of gait. This paper compares four calibration approaches using data from 22 able-bodied subjects walking at 14 speeds [1]. The typical pure centering (PC) approach employed for thigh-based phase variables is not viable, yielding monotonic phase progression in fewer than half of the cases. An optimization (OPT) approach found monotonic calibrations in 305/308 cases with high linearity (average R^2 of 0.91). Critical point centering (CPC) approximates the OPT performance, with 274/308 monotonic calibrations and an average R^2 of 0.85, whereas the related vertical weighted average (VWA) approach was only slightly better than PC. All four approaches are similarly accurate in predicting gait percentage, staying within 5% at least 92.7% of the time.**

I. Introduction

Compared to passive prosthetic legs, robotic lower-limb prostheses have the potential to increase the mobility and functionality of individuals with amputation. Advancing the control of these prostheses is key to realizing their potential. Traditional control of such prostheses using finite-state machines (FSMs) subdivides the gait cycle into discrete states, each with unique control laws based on a series of predefined transition rules [2]. While FSM controllers are highly reliable and repeatable, their discrete nature can result in either sudden actuation that may feel unnatural or misclassifications of the current state that yield improper actuation [3].

Control that is continuous with respect to gait progression has the potential for smoother, more natural feeling actuation. Central pattern generator (CPG) controllers aim for this by applying the CPG phenomena observed in cyclic locomotion in nature [4] to coordinate prosthesis control with either detected gait events [5] or sound-limb motion [6]. Machine learning approaches have also achieved smooth rhythmic control by training neural networks to predict gait progression and output appropriate joint control [7], [8]. While they do provide continuous control throughout gait, these approaches often involve many sensors located off-board the prosthesis [5]–[7] and/or large training data sets [7], [8].

Bipedal robot research introduced a control scheme that characterizes gait progression based on a time-independent phase variable [9], which was later adopted to control lower-limb prostheses [10]–[13]. A phase variable, denoted herein as ϕ, should progress monotonically from 0 to 100% of the gait cycle, and can be used for continuous position [12], [13] or impedance [14] control. The approach relies on accurate estimation of gait progression, as errors in gait percentage prediction can result in poorly timed control, which could lead to higher energy expenditure [15] or falls [16].

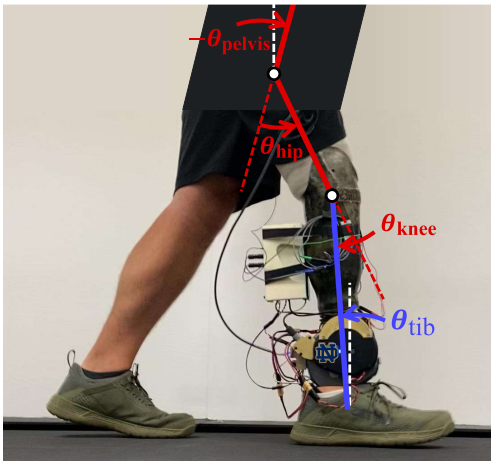

Fig. 1: Global tibia angle (blue) with respect to vertical (white dashed line), calculated from pelvis, hip, & knee kinematics (red).

Candidate phase variables include the foot center of pressure [17], [18] (only able to monitor gait progression in stance) and various hip and thigh kinematics [19], [20]. For transfemoral prostheses, thigh kinematics are preferred, as only sensors onboard the prosthesis are required. For transtibial prostheses, however, thigh-based phase variables require additional sensors on the user's body, increasing donning/doffing requirements. Therefore, a phase variable defined by the global kinematics of the tibia, such as θ_{tib} in Fig. 1, is desirable for transtibial prostheses since sensors onboard the prosthesis could measure it directly [12] (without the need to measure the other kinematic quantities shown in Fig. 1). Here, the global tibia angle is defined as measured in the sagittal plane relative to the gravity-fixed vertical.

Regardless of the phase variable selected, phase-based control requires calibration to determine its relationship to gait progression. Monotonicity in this relationship is critical to avoid one phase variable value ϕ representing multiple gait percentages. Linearity is also important to minimize sensitivity to sensor noise since a linear relationship reduces, across the gait cycle, the change in gait percentage corresponding to a given change in ϕ. To achieve monotonicity and maximize linearity, the phase portrait, which exists on the phase plane defined by global tibia angle (horizontal axis) and tibia angular velocity (vertical axis), must be shifted and

*This work was funded by NSF grants DGE-1841556 & CMMI-1943703.

[1]All authors are with the Department of Aerospace and Mechanical Engineering, University of Notre Dame, Notre Dame, IN 46556, USA rposh@nd.edu

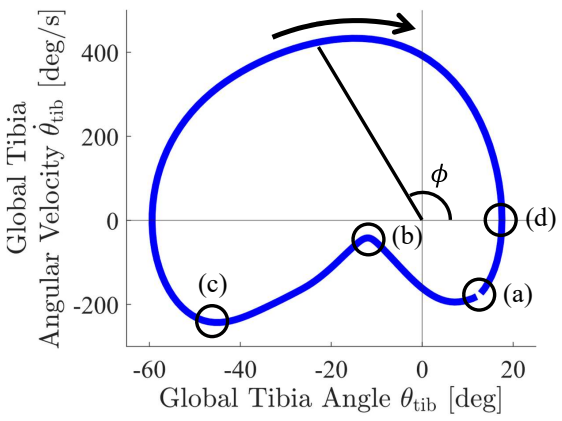

Fig. 2: Average tibia-based phase portrait for subject AB06 walking at 1.8 m/s. Gait cycle begins with heel strike (a), reaches critical point (b) when knee returns to full extension after weight acceptance, enters swing with toe-off (c), & initiates swing leg retraction (d) before beginning again at next heel strike (a).

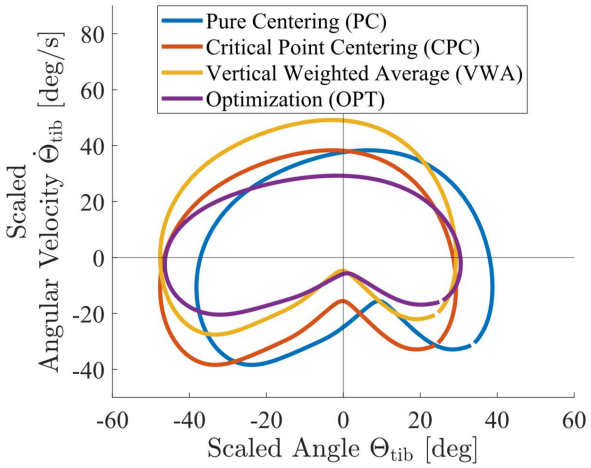

Fig. 3: Average tibia-based phase portrait for subject AB06 walking at 1.8 m/s reparameterized using four calibration approaches.

scaled. For hip-related phase variables, the phase portrait is typically centered about the origin and the data are scaled to ensure that the horizontal and vertical ranges are equal [13].

This paper explores the performance of four calibration approaches to demonstrate the potential of a tibia-based phase variable for control of robotic transtibial prostheses. Two more traditional approaches (pure centering and critical point centering) are assessed alongside two novel approaches (vertical weighted average and optimization). Performance is assessed with data from able-bodied subjects walking on a flat treadmill at a variety of speeds [1]. The monotonicity, linearity, and gait percentage prediction resulting from each calibration approach are compared.

II. Methods

A. Dataset and Processing

Joint kinematics from 22 able-bodied subjects (AB06 - AB30, missing numbers 22, 26, and 29) with mean age 21 years (σ = 4.3 years), mean height 1.7 m (σ = 0.007 m), and mean weight 68.3 kg (σ = 10.83 kg) were collected by [1] at 200 Hz. While all subjects walked on a treadmill with flat orientation for 30 seconds at each of 28 speeds, this work analyzed just the 14 speeds from 0.5 to 1.8 m/s in 0.1 m/s increments. Each combination of subject and speed is called herein a condition (308 total conditions). For each condition, the first half of the strides were used for calibration (Sec. II-C) and the remaining strides for analysis (Sec. II-D).

The kinematics considered include the absolute pelvis tilt angle θ_{pelvis} (positive with posterior tilt), relative hip angle θ_{hip} (positive with hip flexion), and relative knee angle θ_{knee} (positive for knee flexion), all as rotations about a medial-lateral axis and measured from the right leg only, as shown in Fig. 1. The global tibia angle θ_{tib} was calculated as

$$\theta_{\text{tib}} = \theta_{\text{pelvis}} + \theta_{\text{hip}} - \theta_{\text{knee}}. \tag{1}$$

Thus, θ_{tib} is positive when the ankle is in front of the knee. The absolute tibia angular velocity $\dot{\theta}_{\text{tib}}$ was determined by taking the time derivative of θ_{tib} via finite difference. Ground-truth gait percentage data from heel strikes occurring at 0 and 100% of gait cycle were determined when the heel marker's linear velocity became zero [1].

B. Tibia-Based Phase Variable

The tibia-based phase portrait exists on the phase plane consisting of θ_{tib} and $\dot{\theta}_{\text{tib}}$ on the horizontal and vertical axes, respectively, and exhibits the cardioid shape shown in Fig. 2. Heel strike occurs in the bottom right quadrant (Fig. 2(a)), as θ_{tib} is positive and $\dot{\theta}_{\text{tib}}$ is negative due to swing leg retraction [21] (Fig. 2(d)). After heel-strike, the phase portrait progresses clockwise until the next heel strike. Between early- and mid-stance, the tibia velocity decelerates due to the knee extension that occurs when knee loading is complete. This leads to a critical point in the bottom half of the phase portrait (Fig. 2(b)), which is more pronounced at faster speeds. Toe-off occurs near the global minimum of $\dot{\theta}_{\text{tib}}$ (Fig. 2(c)), and swing corresponds to the round portion of the phase portrait in the positive velocity region. The phase variable corresponding to the tibia phase portrait is

$$\phi_{\text{uncalibrated}}(t) = \text{atan2}(\dot{\theta}_{\text{tib}}(t), \theta_{\text{tib}}(t)). \tag{2}$$

Thus, as gait percentage increases from 0 to 100%, the phase variable begin s in the fourth quadrant (270-360 degrees) and progresses clockwise through the phase portrait until beginning again with heel strike.

C. Calibration

To ensure a monotonic relationship between the phase variable and gait percentage, the phase portrait must be scaled and shifted. Calibration parameters x_0, y_0, and k transform the tibia angle and velocity into new variables,

$$\Theta_{\text{tib}}(t) = \theta_{\text{tib}}(t) - x_0 \tag{3}$$
$$\dot{\Theta}_{\text{tib}}(t) = k(\dot{\theta}_{\text{tib}}(t) - y_0), \tag{4}$$

that are used to compute the final phase variable

$$\phi(t) = \text{atan2}(\dot{\Theta}_{\text{tib}}(t), \Theta_{\text{tib}}(t)). \tag{5}$$

Four approaches to obtain the calibration parameters are explored herein, with representative results shown in Fig. 3.

1) Pure Centering (PC): The standard calibration approach for thigh-related phase variables centers the phase portrait about the origin [13]. Thus, PC calibration shifts the tibia-based phase portrait based on the average of the max and min global tibia angles and velocities across all strides.

$$x_0 = (\overline{\theta}_{\text{tib}} + \underline{\theta}_{\text{tib}})/2 \quad (6)$$

$$y_0 = (\overline{\dot{\theta}}_{\text{tib}} + \underline{\dot{\theta}}_{\text{tib}})/2 \quad (7)$$

$$k = \frac{|\overline{\theta}_{\text{tib}} - \underline{\theta}_{\text{tib}}|}{|\overline{\dot{\theta}}_{\text{tib}} - \underline{\dot{\theta}}_{\text{tib}}|}, \quad (8)$$

where $\overline{\theta}_{\text{tib}}$ and $\overline{\dot{\theta}}_{\text{tib}}$ are the maximum global tibia angle and velocity and $\underline{\theta}_{\text{tib}}$ and $\underline{\dot{\theta}}_{\text{tib}}$ are the minimums. Comparing the light blue phase portrait in Fig. 3 to the darker blue one in Fig. 2, PC calibration centers the coordinate system origin within the phase portrait by shifting all values of θ_{tib} and $\dot{\theta}_{\text{tib}}$ by the magnitudes of their geometric centerpoints. The scaling factor k merely adjusts the values of $\dot{\theta}_{\text{tib}}$ such that the axes are evenly scaled.

2) Critical Point Centering (CPC): The tibia-based phase portrait's cardioid shape often prevents monotonicity using PC calibration. Therefore, CPC calibration shifts the phase portrait to place the critical point (Fig 2(b)) on the y-axis [12]. The critical point is defined by the local maximum of $\dot{\theta}_{\text{tib}}$ between heel strike (Fig 2(a)) and toe-off (Fig 2(c)). The corresponding value of θ_{tib} at this peak is used to shift the phase portrait such that the peak lies on the y-axis, as shown by the red phase portrait in Fig. 3. Explicitly, x_0 becomes the value of θ_{tib} corresponding to the maximum global tibia velocity during stance,

$$x_0 = \theta_{\text{tib}}(\max(\dot{\theta}_{\text{tib}_{\text{stance}}})). \quad (9)$$

Equations 7 and 8 are still used to calculate y_0 and k.

3) Vertical Weighted Average (VWA): The phase variable ϕ progresses more slowly during stance than swing. Vertically shifting the phase portrait to move the stance region closer to the origin could reduce the effects of this difference in speed progression and improve linearity. Therefore, VWA calibration shifts the phase portrait horizontally, as in CPC calibration, but it also vertically shifts the portrait by the weighted average of all $\dot{\theta}_{\text{tib}}$ points. The calibration parameter y_0 is calculated as

$$y_0 = \frac{\sum_{n=0}^{N} \dot{\theta}_{\text{tib}}(n)}{n}, \quad (10)$$

where N is the number of collected $\dot{\theta}_{\text{tib}}$ values for a given calibration. By taking the weighted average, y_0 decreases compared to PC and CPC calibrations. Thus, the critical point is nearer to the origin, as shown by the yellow phase portrait in Fig. 3. Equations 8 and 9 are used to obtain k and x_0.

4) Optimization (OPT): To maximize linearity of the relationship between gait percentage and phase variable ϕ while maintaining monotonicity, x_0, y_0, and k were obtained via a grid search optimization. Search ranges were heuristically determined from results of a larger grid search across subjects and speeds. The average θ_{tib} and $\dot{\theta}_{\text{tib}}$ trajectories were computed from the calibration strides. An initial k_0 is calculated by Eq. 6, where the max and min were taken from the mean trajectory. The grid search spanned 26 candidate values for k ($k_0 - 0.1$ to $k_0 + 0.025$, increments of 0.005), 51 values for x_0 (10 to -40 degrees, increments of 1), and 21 values for y_0 (0 to 100 degrees/second, increments of 5).

A monotonicity constraint is enforced so that the derivative of ϕ with respect to gait percentage does not change sign. Linearity is optimized via

$$\begin{aligned} \min_{x_0,y_0,k} \quad & \sum_{p=0}^{100} \left| \frac{\mathrm{d}\phi(x_0,y_0,k,p)}{\mathrm{d}p} - \overline{\frac{\mathrm{d}\phi}{\mathrm{d}p}} \right| \\ \text{s.t.} \quad & \frac{\mathrm{d}\phi}{\mathrm{d}p} < 0, \forall p \in [0, 100], \end{aligned} \quad (11)$$

where $\frac{\mathrm{d}\phi(x_0,y_0,k,p)}{\mathrm{d}p}$ is the derivative of ϕ with respect to the gait percentage p and $\overline{\frac{\mathrm{d}\phi}{\mathrm{d}p}}$ is the average derivative across all p. By minimizing the sum of the absolute differences between the derivative at each gait percentage and the average derivative across all percentages, ϕ trajectories are considered most linear when this cost is closest to 0.

D. Performance Metrics

Once the calibration parameters are determined, the explicit relationship between phase variable ϕ and gait progression is formally established. During subsequent strides, the real-time measurement of ϕ is input to this relationship to yield an output prediction of gait percentage. The utility of the relationship can be evaluated in terms of monotonicity, linearity, and stride-to-stride error.

1) Monotonicity: Evaluation of the constraint in Eq. 11 quantified the monotonicity of the relationship for all approaches. Conditions that violated this constraint were considered non-monotonic and represented a failed calibration.

2) Linearity: A best fit line generated via a linear least squares regression assessed the linearity of the relationship resulting from each calibration. The coefficient of determination (R^2) quantified how well the linear fit model explained the variation in the data.

3) Gait Percentage Prediction: The remaining half of strides for each condition were used to assess how well the calibrated phase variable predicted gait percentage. Differences between the predicted and true gait percentages were considered errors, quantified in percentage of gait.

III. Results and Discussion

Using subject AB06 walking at 1.8 m/s as a representative example, Fig. 5 shows the progression of phase variable ϕ using each calibration approach, and Table I lists the calibration parameters.

A. Monotonicity

The global tibia phase variable's monotonicity depended heavily on the calibration approach. As seen in Fig. 4, PC calibration resulted in less than 44% of the subject-speed conditions (135/308) exhibiting monotonic behavior. This poor performance is due to the critical point in the phase portrait (Fig. 2), which is not present in the near-circular phase portrait of the hip/thigh kinematics often used in control of

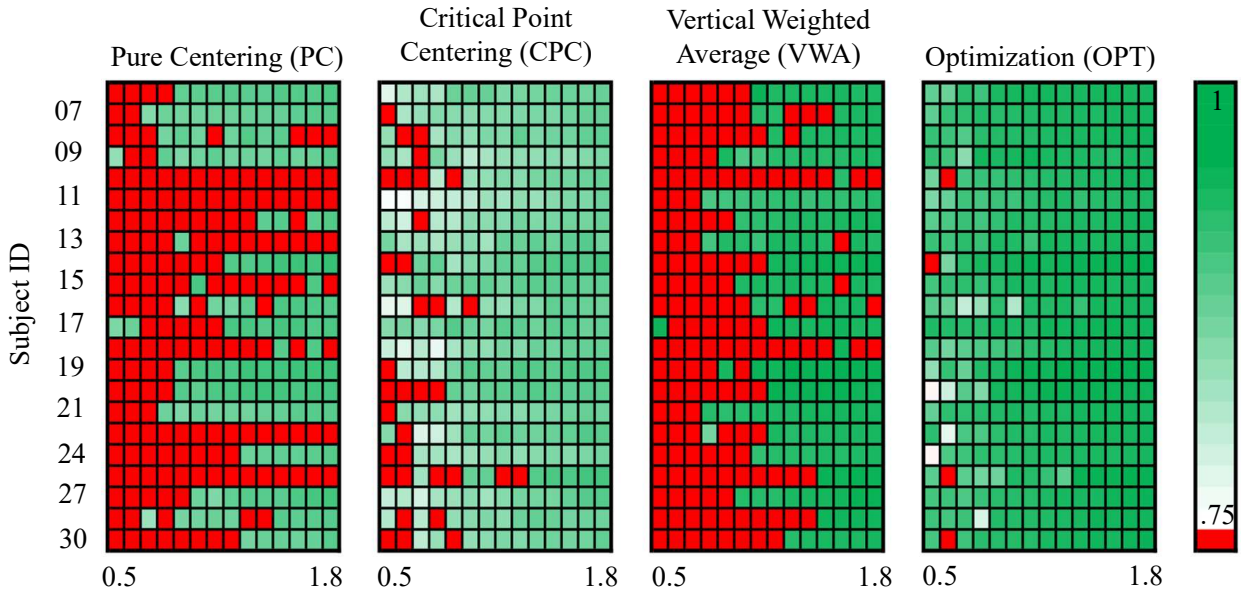

Fig. 4: Monotonicity & linearity. Red squares represent subject & speed conditions without monotonic relationships between phase variable & gait percentage. All other conditions were monotonic, with darker green indicating relationships having R-squared values closer to 1.

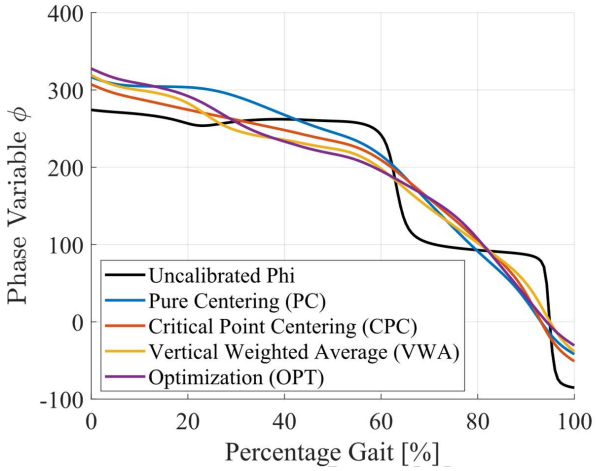

Fig. 5: Progression of calibrated phase variables ϕ for each calibration approach for subject AB06 walking at 1.8 m/s.

transfemoral prostheses [13]. Therefore, for the tibia-based phase variable, PC calibration is not practically viable as the majority of conditions resulted in non-monitinicity, where one value of ϕ corresponds to multiple gait percentages.

CPC calibration places the origin directly above the phase portrait's critical point (Fig. 2b) at a vertical height unchanged from PC calibration. This horizontal shifting resulted in CPC calibration yielding a monotonic relationship between the phase variable and gait percentage in nearly 89% of conditions (274/308). This demonstrates the significance of properly shifting the phase portrait in the horizontal direction to achieve a monotonic relationship.

VWA calibration maintains the origin's horizontal centering relative to the cardiod's critical point as in CPC, but vertically shifts the origin much closer to the critical point, especially at slower speeds. This resulted in far fewer conditions with monotonic relationships, down to approximately

TABLE I: Calibration Parameters for AB06 at 1.8 m/s.

Calibration	x_0	y_0	k
None	0	0	1
PC	-21.23	95.24	0.1135
CPC	-11.78	95.24	0.1135
VWA	-11.78	-0.10	0.1135
OPT	-13	35	0.0735

50% (155/308). This loss of monotonicity was concentrated at slower speeds, with 94.3% of conditions being non-monotonic for speeds between 0.5 and 0.8 m/s. At slower speeds, there was more variation in the global tibia velocity throughout stance, resulting in multiple critical points not always related to knee extension after loading (Fig. 2b). Therefore, VWA calibration more often resulted in ϕ briefly progressing counterclockwise when traversing over the other local peaks in the phase portrait (Fig. 6), making it more sensitive to these minor variations in global tibia speed. While this approach was motivated by improvements in linearity, this lack of monotonic consistency renders VWA calibration undesirable.

OPT calibration yielded a monotonic solution in nearly every condition (98.7%, 304/308). The four conditions without monotonic solutions were at the slowest two speeds, suggesting again that monotonicity is more difficult to achieve at slower speeds. The OPT-generated y_0 was less than the CPC-generated y_0 in 94% of conditions (289/308), but greater than the VWA-generated y_0 for every condition in which OPT achieved monotonicity (304/308), as in Table I. Therefore, when seeking to ensure monotonicity and optimize for linearity, the origin's vertical location lies between those produced by CPC and VWA calibrations. In contrast, the OPT-generated x_0 was on average within 2 degrees of the CPC- and VWA-generated x_0 values for the lowest 4 (0.5-

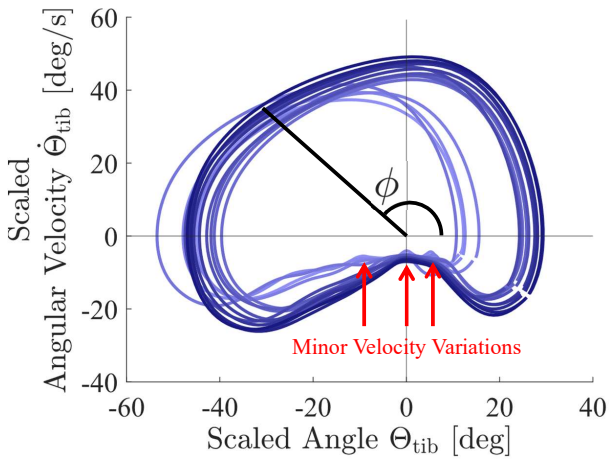

Fig. 6: Average phase portrait for AB18 walking 0.5 m/s (lightest blue) to 1.8 m/s (darkest blue). Low speeds show higher angular velocity variation, which can lead to non-monotonic ϕ progression.

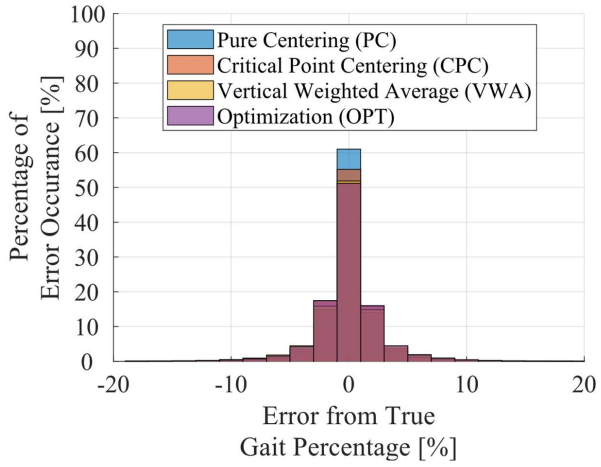

Fig. 7: Frequency of errors between predicted & true gait percentage for all subjects at all speeds. Only errors from conditions with monotonic ϕ progression were considered.

0.8 m/s) and highest 5 speeds (1.4-1.8 m/s). This parameter was within 3 degrees for speeds between 0.9 and 1.3 m/s, where OPT calibration tended to shift the phase portrait farther to the right than CPC and VWA calibrations. For every condition, the OPT-generated scaling parameter k was less than those found by PC, CPC, and VWA calibrations (all of which were equivalent). For all speeds, the OPT-generated k was more than 30% less than that found by PC, CPC, and VWA, and more than 40% less for the lowest 3 speeds (0.5-0.7 m/s). Therefore, scaling such that the vertical range of values is at least 30% less than the horizontal range may be beneficial for monotonicty and linearity.

B. Linearity

In all conditions for which monotonicity was achieved, the linearity of the relationship between the phase variable and gait percentage (Fig. 5) was also assessed. Figure 4 shows the relative linearity of each approach, with dark green indicating conditions for which the relationship had an R^2 value close to 1 and red indicating conditions for which the calibration failed to achieve monotonicity. While PC calibration had an average R^2 value of 0.88, the previously discussed lack of monototonicity renders this approach unviable. The CPC calibration's average R^2 value was 0.85, meaning that 85% of the variation in the relationship could be accounted for by a linear fit. Figure 4 also suggests a relationship between linearity and walking speed for CPC calibration. When comparing linearity and speed, the Pearson correlation coefficient was 0.71, with a p-value of 1.8E-43, indicating that faster speeds resulted in a more linear relationship for CPC calibration.

While like PC calibration in terms of poor monotonicity, VWA calibration in general yielded quite linear phase variable curves, with an average R^2 value of 0.93. This suggests that moving the critical point of the phase portrait closer to the origin yields a more linear result than anticipated, but unfortunately at a high cost to monotonicity. The benefit of a vertical shift is more successfully realized with OPT calibration, where the shift lies between that of CPC and VWA calibrations and results in an average R^2 value of 0.92 (also between that of CPC and VWA calibrations). The speed/linearity relationship observed in CPC calibration is less pronounced with both VWA (Pearson correlation of 0.50, p-value 4.7E-11) and OPT (Pearson correlation of 0.61, p-value 1.8E-32) calibrations. This is likely due to the fact that most of the speeds that were monotonic showed similarly high linearity, regardless of speed.

Overall, the location of the critical point is crucial for achieving both monotonicity and linearity. Shifting the critical point horizontally to lie on the vertical axis is key for monotonicity in general. Shifting it vertically toward the origin can increase linearity, but when too close to the origin, monotonicity can be compromised. According to OPT calibration, the optimal vertical shift lies between those of the CPC and VWA calibrations. Identifying a reliable heuristic to achieve this optimal shift is a topic of future research.

C. Gait Percentage Prediction

For control purposes, once calibration is complete, the established relationship between the phase variable and gait percentage is used to predict the gait percentage of future strides based on real-time sensor measurement of the phase variable (likely an IMU on the transtibial prosthesis). Using only the second half of strides from each condition (not included for calibration), Fig. 7 shows a histogram of the prediction errors in gait percentage for all 4 approaches for conditions that were monotonic. Despite differences in monotonicity and linearity overall, the four approaches show similar performance in prediction error. OPT calibration, for example, has approximately 50% of all errors observed within $\pm$ 1% of the true gait percentage. All approaches have at least 92.7% of all errors observed within 5% of gait, and 99.9% of errors within 13% of gait. As these errors only consider conditions that were monotonic, calibrations that are not monotonic would result in large prediction errors, as one value of ϕ corresponds to multiple gait percentages.

Figure 8 shows an example of the predicted gait percentage from OPT calibration compared to the true gait

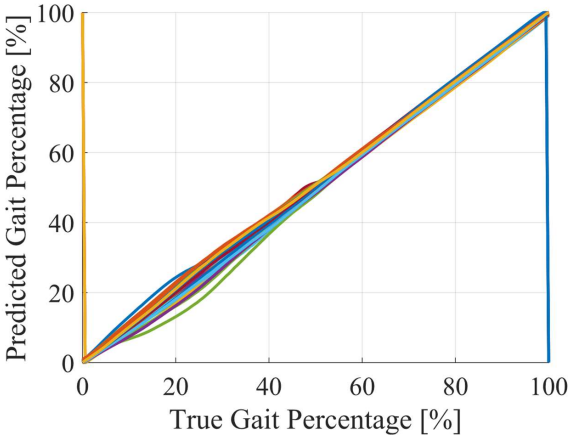

Fig. 8: Predicted (from optimization) versus true gait percentage for AB06 walking at 1.8 m/s (22 strides). Large errors near 0 & 100% of gait were treated as small errors relative to adjacent strides.

percentage for 22 strides of subject AB06 walking at 1.8 m/s. Consistent with all subjects, nearly all errors occur during stance (less than ∼60% of gait cycle), with the largest magnitudes near 20% of gait cycle, which corresponds to the location of the critical point of the phase portrait (Fig. 2b). Echoing the monotonicity and linearity results, this again highlights the importance of calibration, with the key factor being the location of the origin relative to the critical point.

IV. Conclusions

The global tibia kinematics can be used to define a phase variable for monitoring gait cycle progression for control of robotic transtibial prostheses. Calibration of this phase variable can be achieved by having individuals with amputation walk for 10-20 strides. From such strides, this paper examines calibration via four approaches across a range of speeds. Of the four, the optimization (OPT) approach not surprisingly offers the best combination of monotonicity, linearity, and error performance. When linearity is less of a priority, however, the critical point centering (CPC) approach is an appropriate substitute, especially for speeds above 0.7 m/s. While the pure centering (PC) approach has been useful for thigh-related phase variables, the cardioid shape of the tibia-based phase portrait renders it unviable for tibia-related phase variables. The vertical weighted average (VWA) approach increased the linearity of the relationship between the phase variable and gait percentage compared to CPC calibration, but led to frequent failed calibrations due to non-monotonicity. Accuracy of gait percentage prediction was similar across all four calibration approaches. Having a phase variable calibration curve that is monotonic, nearly linear, and accurate in prediction is critical for new control approaches, such as phase-based impedance control within hybrid volitional control frameworks [22]. Future work will seek to validate these calibration approaches with hardware.

References

[1] J. Camargo, A. Ramanathan, W. Flanagan, and A. Young, "A comprehensive, open-source dataset of lower limb biomechanics in multiple conditions of stairs, ramps, and level-ground ambulation and transitions," *J Biomech*, vol. 119, p. 110320, 2021.

[2] F. Sup, A. Bohara, and M. Goldfarb, "Design and control of a powered knee and ankle prosthesis," *IEEE Int Conf Robot Autom*, pp. 4134–4139, 2007.

[3] R. R. Posh, J. P. Schmiedeler, and P. M. Wensing, "Finite-state impedance and direct myoelectric control for robotic ankle prostheses: Comparing their performance and exploring their combination," *IEEE T Neur Sys Reh*, vol. 31, pp. 2778–2788, 2023.

[4] A. J. Ijspeert, "Central pattern generators for locomotion control in animals and robots: a review," *Neural Networks*, vol. 21, no. 4, pp. 642–653, 2008.

[5] R. R. Torrealba, J. Cappelletto, L. Fermín, G. Fernández-López, and J. C. Grieco, "Cybernetic knee prosthesis: application of an adaptive central pattern generator," *Kybernetes*, vol. 41, no. 1/2, pp. 192–205, 2012.

[6] J.-K. Ryu, N. Y. Chong, B. J. You, and H. Christensen, "Adaptive cpg based coordinated control of healthy and robotic lower limb movements," *IEEE Int Symp Robot Human Interact Commun*, pp. 122–127, 2009.

[7] I. Kang, D. D. Molinaro, S. Duggal, Y. Chen, P. Kunapuli, and A. J. Young, "Real-time gait phase estimation for robotic hip exoskeleton control during multimodal locomotion," *IEEE Robot Autom Lett*, vol. 6, no. 2, pp. 3491–3497, 2021.

[8] H. T. T. Vu, F. Gomez, P. Cherelle, D. Lefeber, A. Nowé, and B. Vanderborght, "ED-FNN: A new deep learning algorithm to detect percentage of the gait cycle for powered prostheses," *Sensors*, vol. 18, no. 7, p. 2389, 2018.

[9] E. R. Westervelt, J. W. Grizzle, C. Chevallereau, J. H. Choi, and B. Morris, *Feedback Control of Dynamic Bipedal Robot Locomotion*. CRC press, 2018.

[10] H. L. Bartlett and M. Goldfarb, "A phase variable approach for imu-based locomotion activity recognition," *IEEE T Biomed Eng*, vol. 65, no. 6, pp. 1330–1338, 2017.

[11] R. D. Gregg, T. Lenzi, L. J. Hargrove, and J. W. Sensinger, "Virtual constraint control of a powered prosthetic leg: From simulation to experiments with transfemoral amputees," *IEEE T Robot*, vol. 30, no. 6, pp. 1455–1471, 2014.

[12] M. A. Holgate, T. G. Sugar, and A. W. Bohler, "A novel control algorithm for wearable robotics using phase plane invariants," *IEEE Int Conf Robot Autom*, pp. 3845–3850, 2009.

[13] D. Quintero, D. J. Villarreal, D. J. Lambert, S. Kapp, and R. D. Gregg, "Continuous-phase control of a powered knee–ankle prosthesis: Amputee experiments across speeds and inclines," *IEEE T Robot*, vol. 34, no. 3, pp. 686–701, 2018.

[14] T. K. Best, C. G. Welker, E. J. Rouse, and R. D. Gregg, "Data-driven variable impedance control of a powered knee–ankle prosthesis for adaptive speed and incline walking," *IEEE T Robot*, 2023.

[15] P. Malcolm, R. E. Quesada, J. M. Caputo, and S. H. Collins, "The influence of push-off timing in a robotic ankle-foot prosthesis on the energetics and mechanics of walking," *J Neuroeng Rehabil*, vol. 12, no. 1, pp. 1–15, 2015.

[16] M. Riveras, E. Ravera, D. Ewins, A. F. Shaheen, and P. Catalfamo-Formento, "Minimum toe clearance and tripping probability in people with unilateral transtibial amputation walking on ramps with different prosthetic designs," *Gait Posture*, vol. 81, pp. 41–48, 2020.

[17] R. D. Gregg, T. Lenzi, N. P. Fey, L. J. Hargrove, and J. W. Sensinger, "Experimental effective shape control of a powered transfemoral prosthesis," *IEEE Int Conf Rehabil Robot*, pp. 1–7, 2013.

[18] R. D. Gregg and J. W. Sensinger, "Towards biomimetic virtual constraint control of a powered prosthetic leg," *IEEE T Control Syst Technol*, vol. 22, no. 1, pp. 246–254, 2013.

[19] D. J. Villarreal and R. D. Gregg, "A survey of phase variable candidates of human locomotion," *IEEE Int Conf Eng Med Biol Soc*, pp. 4017–4021, 2014.

[20] R. J. Cortino, E. Bolívar-Nieto, T. K. Best, and R. D. Gregg, "Stair ascent phase-variable control of a powered knee-ankle prosthesis," *IEEE Int Conf Robot Autom*, pp. 5673–5678, 2022.

[21] K. Poggensee, M. Sharbafi, and A. Seyfarth, "Characterizing swing-leg retraction in human locomotion," *17th Int Conf Climbing Walking Robots (CLAWAR)*, pp. 377–384, 2014.

[22] R. R. Posh, J. P. Schmiedeler, and P. M. Wensing, "Hybrid volitional control as a framework for lower-limb prosthetic control: A simulation study," *IEEE Int Conf Intell Robots Syst*, pp. 6167–6163, 2021.